



Vibration characteristics of marine riser groups considering the coupled action of cross-flow and in-line

Xiaohong Zhang¹ · Xiaoqiang Guo^{2,3} · Liming Dai³ · Jun Liu² · Guorong Wang²

Received: 7 October 2020 / Accepted: 13 January 2021 / Published online: 2 February 2021
© Saudi Society for Geosciences 2021

Abstract

Fluid-induced vibration (FIV) prediction is an important prerequisite work in wear and fatigue analysis of multi-wellhead marine risers in deepwater operation condition. A two-way fluid-structure coupling method (CFD/CSD) is used to establish a numerical model vibration of the marine riser groups, taking into account the interaction between two physical fields of fluid-structure, the combined effects of ocean eddy-induced force and wave-induced force. The model is solved numerically by ANSYS Workbench and Fluent software and verified preliminarily by a classical example in literature in which considering vibration response of a single riser. The effects of number, spacing, and arrangement of risers on the vibration response characteristics of marine riser groups are analyzed by established mode. It is found that with the increase of the number of risers, the vibration of the front risers is mainly cross-flow (CF), while the vibration of the rear risers is mainly in-line (IL). Therefore, the influence of incoming flow should be taken into account in the front risers, and the disturbance of wake should be taken into account in the rear risers. With the increase of the distance between risers, the interaction between risers groups affects CF and IL. The critical spacing of the interaction is between 3.5D and 4D. The arrangement of marine risers mainly affects the CF vibration of risers, especially the upstream and downstream risers. The research results can provide theoretical support for the design and vibration control of multi-wellhead marine risers.

Keywords FIV · Marine riser groups · Numerical simulation · Fluid-structure coupling · Vibration characteristic

Introduction

In order to improve the efficiency of offshore oil and gas production, it is necessary for deepwater production systems to adapt to wave environments with long oscillation period. The key component in the system is the riser group (Fig. 1). Because the deepwater riser group is shaped as a slender duct, coupled motion in the forward and lateral directions under the combined action of wind, waves, and current on the surface of

the water, as well as fluid within the runner, makes the runner prone to fatigue failure, displacement, and uplift (Fig. 2), requiring periodic repairs and causing serious economic losses.

Research on flow-induced vibration in multi-wellhead marine riser groups remains sparse. Some results have been obtained in studies on one or two pipes. Regarding the single riser, the author has carried out theoretical (Antoine and Sigrist 2009) and experimental research (Griffin and Ramberg 1982), establishing a pipeline flow-induced vibration model and experimentally verifying its accuracy, finding frequency locking in the forward and lateral directions, and laying the foundations for later research. In order to analyze the effects of ocean load on the riser, Xu et al. (2017) used an existing vortex-induced vibration model to research the effects of out-flow velocity, top-end tension, and pipe diameter on lateral flow vibrations. He et al. (2017) used a slender rod model to study the effect of velocity conversion on lateral flow vibrations under uniform flow. Jauvtis and Williamson (2003) showed that the forward vibrations are not negligible when the mass ratio < 6.0. Chaplin et al. (2005) conducted flexible cylinder vortex-induced vibration experiments, showing that the vibration mode and frequency for forward vibration are generally

This article is part of the Topical Collection on *Data Science for Ocean Data Visualization and Modeling*.

✉ Xiaoqiang Guo
786526101@qq.com

¹ School of Computer Science, Southwest Petroleum University, Chengdu 610500, China

² School of Mechatronic Engineering, Southwest Petroleum University, Chengdu 610500, China

³ Industrial Systems Engineering, University of Regina, Regina, SK S4S 0A2, Canada



Fig. 1 Multi-wellhead marine riser group

twice that of lateral flow. Gu et al. (2016), Sang et al. (2019), and Gao et al. (2019) used numerical analysis to study the vortex-induced vibration characteristics of rigid cylinders, showing that the effects of forward-flow vibrations on the riser are highly significant. For flow-induced vibration with two risers, Zdravkovich (1997) analyzed the interference between two cylinders, laying the foundation for interference analysis of multiple structures under the action of fluids. This model only considered the action of flow fields on the structures, ignoring the structures' reaction upon the fluid field. Due to the complexity of the coupling between multiple structures and the flow field, most scholars have used numerical simulation for research. Huse and Kleiven (2000) used a combination of simulation and experiment to analyze the flow-induced vibration characteristics of the riser in response to the spacing problem of mutual interference between the tension-tensioned risers (TTR) of the tension leg platform under uniform and constant flow velocity, verifying the validity of the numerical method. Later, a number of scholars used computers to research flow-induced riser vibration. Huang (2010) and Yan (2010), using



Fig. 2 Marine riser uplift

two marine production risers as research objects, used finite element software to build numerical models, both reaching consistent conclusions under the same sensitivity factors. Zhang et al. (2012), using ABAQUS finite element software, simulated the response of the wave splash zone and the lower zone of the riser under the combined action of waves and platforms and analyzed the sensitivity to a certain degree. Shi et al. (2015) used the commercial program OrcaFlex to analyze interference and the sensitivity towards drag force and top-end tension for TTRs. Zhu et al. (2015) and Song et al. (2016) established a finite element model of differential motion equations for the serial risers of TLP platforms and studied the interference on serial risers under various conditions. Zhou et al. (2016) used a nonlinear 3D beam element, combined with a Huse wake model and “tube-in-tube” model to study the interference on TTR under the action of extremely short waves using finite element simulation.

Thus, most current research involves flow-induced vibration analysis on single or double risers, and none considers the coupled action of forward and lateral flow. Most studies have used unidirectional fluid-solid coupling in numerical simulation of marine risers, without considering the effects of the riser on the flow field. As a result, the accuracy of the calculations has not met the requirements of onsite research. Therefore, this study applies bidirectional fluid-solid coupling, combined with ANSYS Workbench and Fluent analysis software, to establish a numerical model considering the coupled flow of the riser group along both the forward and lateral flow directions and analyzes the effects of riser number, their spacing, and arrangement of groups on their vibration response characteristics.

Numerical model of multi-wellhead marine riser group

Model of riser group vibration

Breuer (1998) found that a distance of πD in the axial direction of the riser (where D is the outer diameter) can reflect the 3D characteristics of the flow field vortex radiation in single riser systems. Therefore, the axial lengths of all riser groups are taken as πD . The model is shown in Fig. 3, using the following assumptions:

- (1) A string constraint is applied to both ends of the riser micro-elements.
- (2) The axial movement of the riser is not considered.
- (3) The external fluid flow is uniform.

This study mainly considers FIV of the riser group under uniform flow—the geometric model is shown in Fig. 4. The

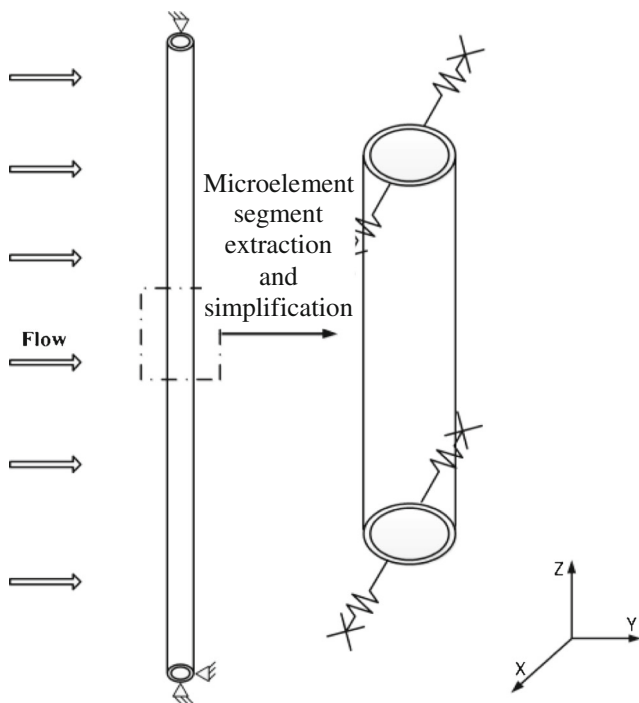


Fig. 3 Simplified single riser model

riser has an outer diameter (D) of 500 mm and axial length (L) of 1600 mm. The group is comprised of 9 independent risers, whose motion can be approximated as elastic bodies and are free to vibrate under uniform flow.

Using the finite element method to discretize the structure, the risers are simulated by solid 3D elements. Each unit node has 6 degrees of freedom, and fixed constraint boundary conditions are used for both ends of the risers. The load calculated from the fluid is added to the unit node in vector form. The dynamic discrete structure equilibrium equation for each riser can be obtained at a given time, considering the coupled action of forward and lateral flow, as shown in reference Liu et al. (2019), Ge et al. (2019), and Liu et al. (2020):

$$\mathbf{M}\ddot{\mathbf{x}} + \mathbf{C}\dot{\mathbf{x}} + \mathbf{K}\mathbf{x} = \mathbf{F}(t) \tag{1}$$

where \mathbf{M} , \mathbf{C} , and \mathbf{K} are the riser mass matrix, damping matrix, and stiffness matrix, respectively. Rayleigh damping

is used, i.e., $\mathbf{C} = \alpha\mathbf{M} + \beta\mathbf{K}$, where α and β indicate the damping coefficients of the structure, respectively; \mathbf{x} , $\dot{\mathbf{x}}$, and $\ddot{\mathbf{x}}$ indicate the displacement, velocity, and acceleration vector of the node, respectively; and $\mathbf{F}(t)$ is the load caused by fluid motion. Using the Newmark algorithm to solve the riser dynamics Eq. (1), the dynamic response of the riser can be obtained.

Marine fluid turbulence model

This paper mainly studies the fluid-solid coupling dynamic behavior and flow field vortex radiation characteristics of multi-wellhead marine riser groups. In order to meet the calculation accuracy conditions, large eddy simulation (LES) is selected as the numerical simulation model to simulate the turbulence of the flow field. The specific analysis follows.

(1) Fluid equations

The fluid in this study is water. The flow rate is low, and it is treated as an incompressible fluid. The equation governing incompressible fluids is the Navier-Stokes (N-S) equation, expressed in Cartesian coordinates (as shown in reference Su and Huang (1997)) as follows:

Continuity equation:

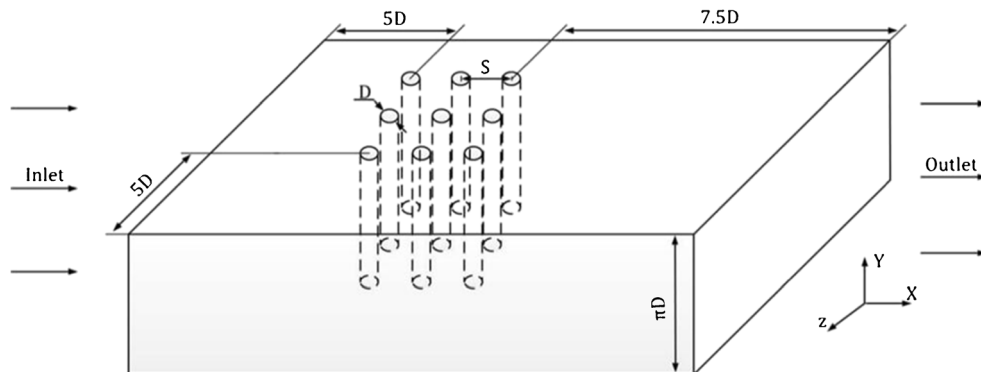
$$\frac{\partial u_i}{\partial x_i} = 0 \tag{2}$$

Conservation of momentum equation:

$$\frac{\partial u_i}{\partial t} + \frac{\partial u_i u_j}{\partial x_j} = -\frac{1}{\rho} \frac{\partial p}{\partial x_i} + \frac{\partial}{\partial x_j} \left(\frac{\mu}{\rho} \frac{\partial u_i}{\partial x_j} \right) \tag{3}$$

where ρ is the fluid density (kg/m^3); t is time (s); p is pressure (pa); μ is dynamic viscosity (pa·s); u_i ($i = 1, 2, 3$) are the velocity components (m/s); and x_i ($i = 1, 2, 3$) are the coordinate components.

Fig. 4 Structural diagram of geometric model



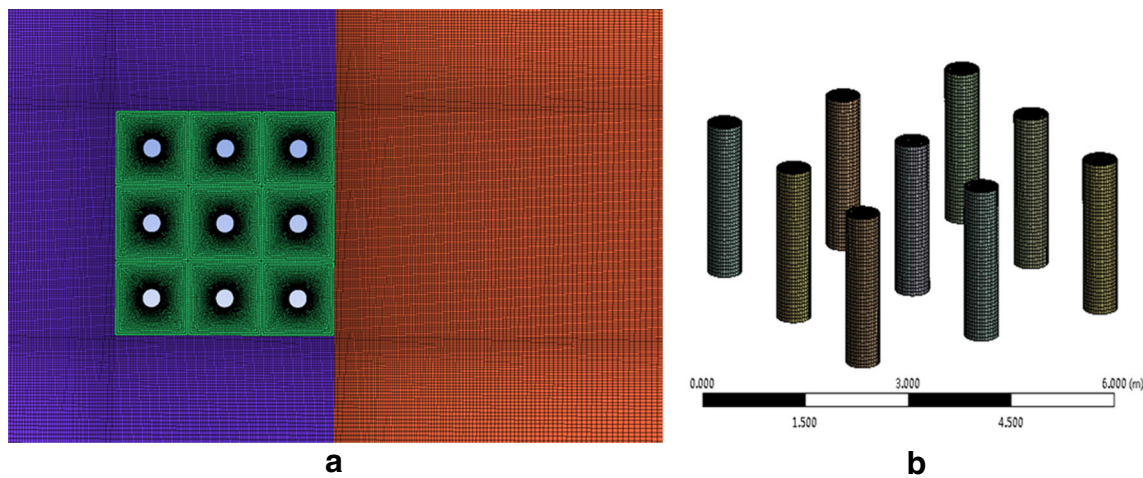


Fig. 5 Model meshing. (a) Flow field. (b) Riser group

The continuity equation and the conservation of momentum equation have similar forms of expression. To this end, the global flow field variable Φ is introduced, so the general motion equation of the fluid equation can be expressed as:

$$\frac{\partial(\rho\Phi)}{\partial t} + \text{div}(\rho\mathbf{u}\Phi) = \text{div}(\Gamma\cdot\text{grad}\Phi) + S \tag{4}$$

where u is the velocity vector (m/s), Φ is the flow field flux, Γ is the diffusion coefficient, and S is the source. If Φ takes different field variables, and an appropriate diffusion coefficient and source are selected, then equations with different physical interpretations (including the continuity and conservation of momentum) will be obtained.

(2) Turbulence simulation

LES (Zhang et al. 2005) is used here to solve for the turbulent flow field. The idea of LES is that large-scale impulses are calculated using direct simulation, while only the effects of small-scale ones on large-scale motion are modeled. The equations governing large-scale eddies can be obtained by filtering the N-S equation in the physical space:

$$\frac{\partial \bar{u}_i}{\partial x_i} = 0 \tag{5}$$

$$\frac{\partial \bar{u}_i}{\partial t} + \frac{\partial \bar{u}_i \bar{u}_j}{\partial x_j} = -\frac{1}{\rho} \frac{\partial \bar{p}}{\partial x_i} + \frac{\partial}{\partial x_j} \left(\frac{\mu}{\rho} \frac{\partial \bar{u}_i}{\partial x_j} \right) - \frac{\partial \tau_{ij}}{\partial x_j} \tag{6}$$

where τ_{ij} is the subgrid-scale stress (Pa), $\tau_{ij} = \bar{u}_i u_j - \bar{u}_i \bar{u}_j$. The subgrid stress generated by the filtering operation is unknown and must be modeled. The subgrid turbulent stress can be calculated in vortex form from the Boussinesq hypothesis:

$$\bar{\tau}_{ij} - \frac{1}{3} \tau_{kk} \delta_{ij} = -2 \left(\mu_t \bar{S}_{ij} \right) \tag{7}$$

where μ_t is the turbulent viscosity of the subgrid, and \bar{S}_{ij} is its strain rate tensor, defined as $\bar{S}_{ij} = \frac{1}{2} \left(\frac{\partial \bar{u}_i}{\partial x_j} + \frac{\partial \bar{u}_j}{\partial x_i} \right)$. The wall-modeled LES (WMLES) subgrid stress model is used, combining a mixed-length model, Smagorinsky model, and wall function to overcome the limitations of LES and the Reynolds number. WMLES can be applied to similar grid resolutions but with higher Reynolds number. The eddy viscosity coefficient is calculated as:

$$\mu_t = \min \left[(\kappa d_w)^2, (C_{\text{Smag}} \Delta)^2 \right] \cdot S \cdot \left\{ 1 - \exp \left[-\left(y^+ / 25 \right)^3 \right] \right\} \tag{8}$$

where $\kappa = 0.41$, d_w is the distance from the wall, $\Delta = \min(\max(C_w \cdot d_w; C_w \cdot h_{\text{MAX}}, h_{\text{wn}}); h_{\text{MAX}})$, S is the strain

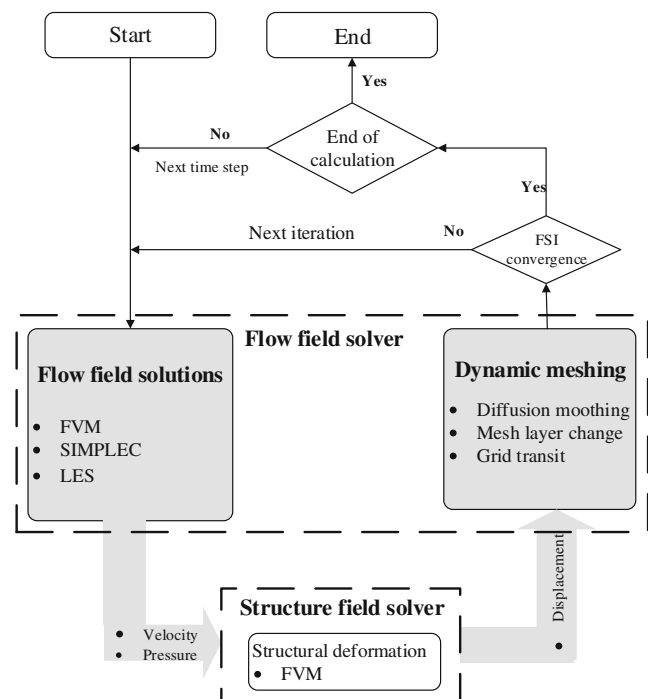
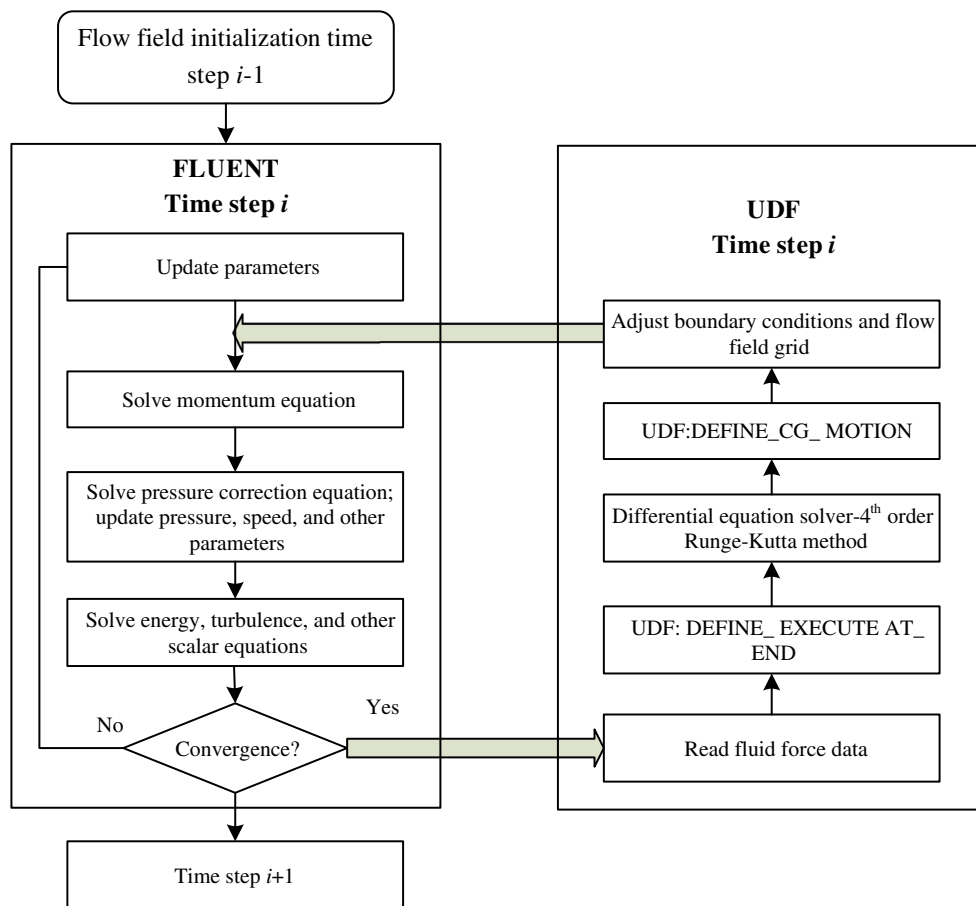


Fig. 6 Fluid-structure coupled iteration process

Fig. 7 Process diagram to solve the fluid-solid coupling problem using Fluent



rate, $C_{Smag} = 0.2$, h_{MAX} is the maximum unit vortex length, h_{wn} is the grid spacing of the wall in the normal direction, and $C_w = 0.15$.

(3) Numerical method to solve flow field

The finite volume method is currently the most widely used method in computational fluid dynamics. The discrete equations obtained by this method conserve the original differential equations better than in other numerical calculation methods and have clear physical interpretations. The requirements for calculation grid shape are not too stringent, and the specification in equation form is advantageous. The key step in this method is to integrate the motion equation with within the control volume as an integral, as follows:

$$\frac{\partial}{\partial t} \int_V \rho \Phi dV + \int_A n \cdot (\rho \mathbf{u} \Phi) dA = \int_A n \cdot (\Gamma \text{grad} \Phi) dA + \int_V S_\Phi dV \quad (9)$$

For the flux Φ , if the boundary of any control body moves, the transit equation, expressed as an integral, is:

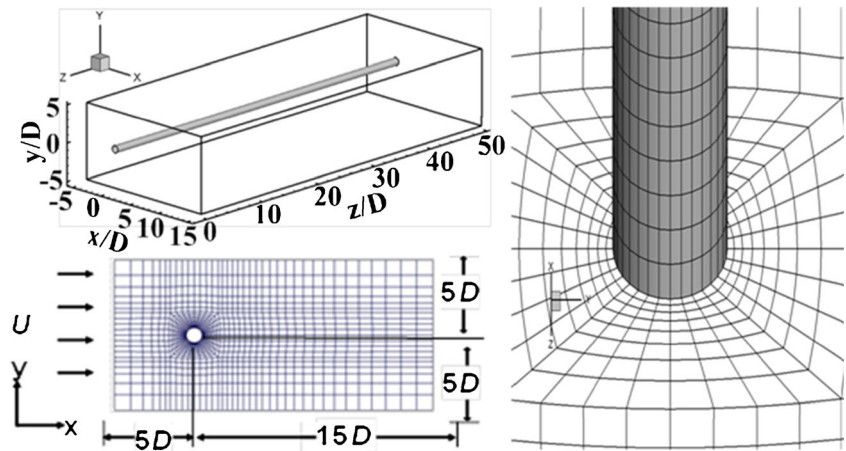
$$\frac{d}{dt} \int_V \rho \Phi dV + \int_A \rho \Phi (\mathbf{u} - \mathbf{u}_s) \cdot dA = \int_A \Gamma \nabla \Phi \cdot dA + \int_V S_\Phi dV \quad (10)$$

where V is the control volume (m^3), ρ is the fluid density (kg/m^3), u is the fluid velocity vector (m/s), u_s is the deformation speed of the dynamic mesh (m/s), A is the surface area of the control body (m^2), S_Φ is the flux source, and Γ is the diffusion coefficient.

Table 1 Physical parameters of riser and fluid

Parameter	Value	Parameter	Value	Parameter	Value
Elastic modulus E (Pa)	10^{10}	Riser density ρ_s (kg/m^3)	6500	Internal fluid density ρ_i (kg/m^3)	850
Outer diameter of riser D (m)	0.01	Riser length L (m)	0.5	External fluid density ρ (kg/m^3)	998
Inner diameter of riser D_i (m)	0.0095	Poisson's ratio ν	0.3	Fluid viscosity ν (pa-s)	0.001

Fig. 8 Diagram of single riser flow field and local meshing



The first term in Eq. (10) can be expressed as a first-order backward difference:

$$\frac{d}{dt} \int_V \rho \Phi dV = \frac{(\rho \Phi V)_{n+1} - (\rho \Phi V)_n}{\Delta t} \quad (11)$$

n and $n+1$ represent the current and subsequent time steps. The volume of step $(n+1)$ V_{n+1} can be obtained by:

$$V_{n+1} = V_n + \frac{dV}{dt} \Delta t \quad (12)$$

The CFD program Fluent, based on the finite volume method, is used to discretize the equations governing the fluid and turbulence model into algebraic equations that can be solved numerically. After discretization, Eq. (9) can be expressed as:

$$a_i \Phi_i = \sum_{j=1}^{N_i} b_j \Phi_{ij} + S_i \quad (13)$$

where Φ_i is flow field flux of the i^{th} control body node; Φ_{ij} is the flow field flux of surface j of the i^{th} control body; S_i is the source; a_i an undetermined coefficient; b_i is flux correlation coefficient of the control body surfaces; and N_i is the number of surfaces on the i^{th} control body. The SIMPLEC algorithm is used for pressure-velocity coupling. The pressure term is discretized in second-order form to improve the accuracy,

the bounded center difference method, based on NVD (Leonard 1991), and the convection bounded criteria are used for momentum dispersion. This method combines the accuracy and convergence of the central difference method and the second- and first-order upwind schemes.

Similar equations can be written for each element in the grid, resulting in an algebraic equation with a sparse coefficient matrix. The Gauss-Seidel linear equation solver and algebraic multigrid (AMG) method are connected to solve this linear system and to obtain unknowns in the flow field such as speed and pressure.

Computational grid generation

The model uses the fluid analysis software Fluent and the structural analysis software Transient Structural to divide the ocean flow and riser group structure fields into units. Dynamic meshing techniques like diffusion smoothing and dynamic mesh layer transformation are also adopted.

The mesh transit in the diffusion smoothing method is governed by the diffusion equation in Eq. (14):

$$\nabla \cdot (\gamma \nabla \mathbf{u}_s) = 0 \quad (14)$$

Fig. 9 Changes in vibration response with U_r : comparison of numerical calculations with experimental result. (a) Response frequency. (b) Lateral amplitude

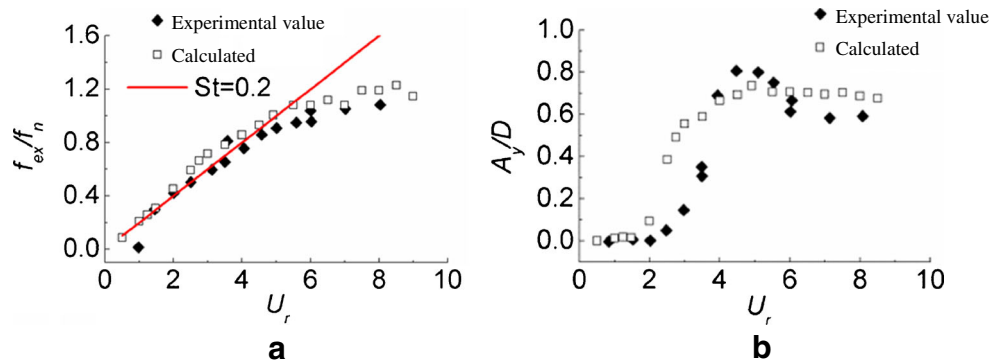
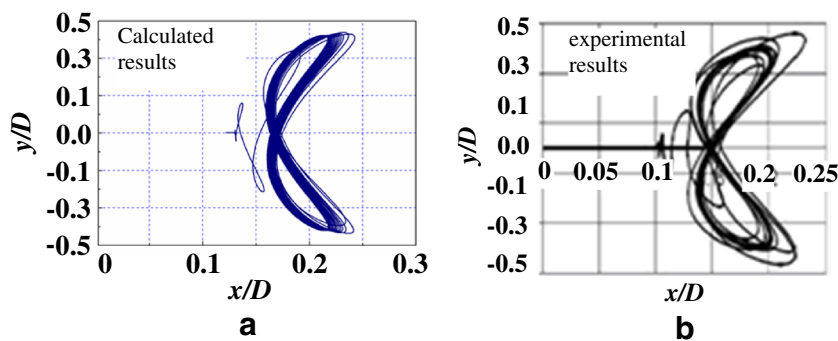


Fig. 10 Motion trajectory. (a) Calculation result. (b) Experimental result



where ∇ is the Laplace operator and \mathbf{u}_s is the grid transit speed; the transit of the mesh on the deformation boundary is tangent to the boundary. Γ is the diffusion coefficient, represented as a unit volume function. $\gamma = 1/V^\alpha$, used to control the effect of the mesh boundary on the internal meshes. α is a control parameter, set here at 2. The transit speed at unit center \mathbf{u}_s is interpolated to each mesh node using distance weighted average, and the node position is updated based on Eq. (15):

$$\mathbf{x}_{\text{new}} = \mathbf{x}_{\text{old}} + \mathbf{u}_s \Delta t \tag{15}$$

For changes in the dynamic mesh layers, the dynamic mesh model specifies an ideal height h_{ideal} . When the grid cell height $h > (1 + \alpha_h)h_{\text{ideal}}$, the cell splits according to the predefined condition; when $h < \alpha_h h_{\text{ideal}}$, the compressed unit layer is merged with the adjacent one, where α_h is the merge/split factor of the global unity layer. Figure 5 respectively shows the flow field and group structure of the 9 risers when arranged as a square.

Fluid-solid coupling calculation

Two-way coupling is essential to solve for the fluid-riser group interaction between the groups. The coupling is realized through iterative riser group dynamics and fluid calculations using the same time step. The data transfer between the structure and fluid domains is carried out through the fluid-solid coupling interface. CSD specifies the deformation in the fluid domain by

calculating structural displacement, while CFD is used to calculate the load acting upon the structure. When the iteration of the fluid and structure domains converge, the calculation at the next time step is started; the loop is repeated until the calculation ends, as follows:

- (1) The Newmark algorithm is used to solve the structural dynamics equation and obtain parameters such as the displacement and velocity of the structure, which are passed to the dynamic grid solver.
- (2) The dynamic grid solver updates the fluid domain mesh based on the structural displacement.
- (3) The CFD solution is used to obtain flow field parameters such as velocity and pressure fields, and the fluid load acting on the structure is transmitted to the structure solver.
- (4) Return to (1) for the next time step.

Although the fluid force is not a continuous function, the fluid solver obtains an instantaneous value at the end of each time step, thereby updating the current structure position and obtaining a fluid calculation grid for the next time step. Figure 6 shows a flow chart of the fluid-structure coupled iterative method.

The coupling between the fluid and the marine riser group is achieved through an embedded user-defined function (UDF) interface. The UDF is the key to fluid-solid coupling using Fluent, and the framework Fluent is used to provide

Table 2 Model calculation parameters

Parameter	Value	Parameter	Value	Parameter	Value
Elastic modulus (Pa)	2.06×10^{11}	Riser density (kg/m^3)	7850	Flow fluid density (kg/m^3)	1000
Outer diameter of riser (m)	0.5	Damping factor α (Schowalter et al. 2006)	5.098	Riser spacing (m)	$2.5D-5D$
Inner diameter of riser (m)	0.3	Damping factor β (Schowalter et al. 2006)	0.000215	Fluid viscosity (pa·s)	0.001
Riser length (m)	1.6	Poisson's ratio ν	0.3	Fluid velocity (m/s)	0.8

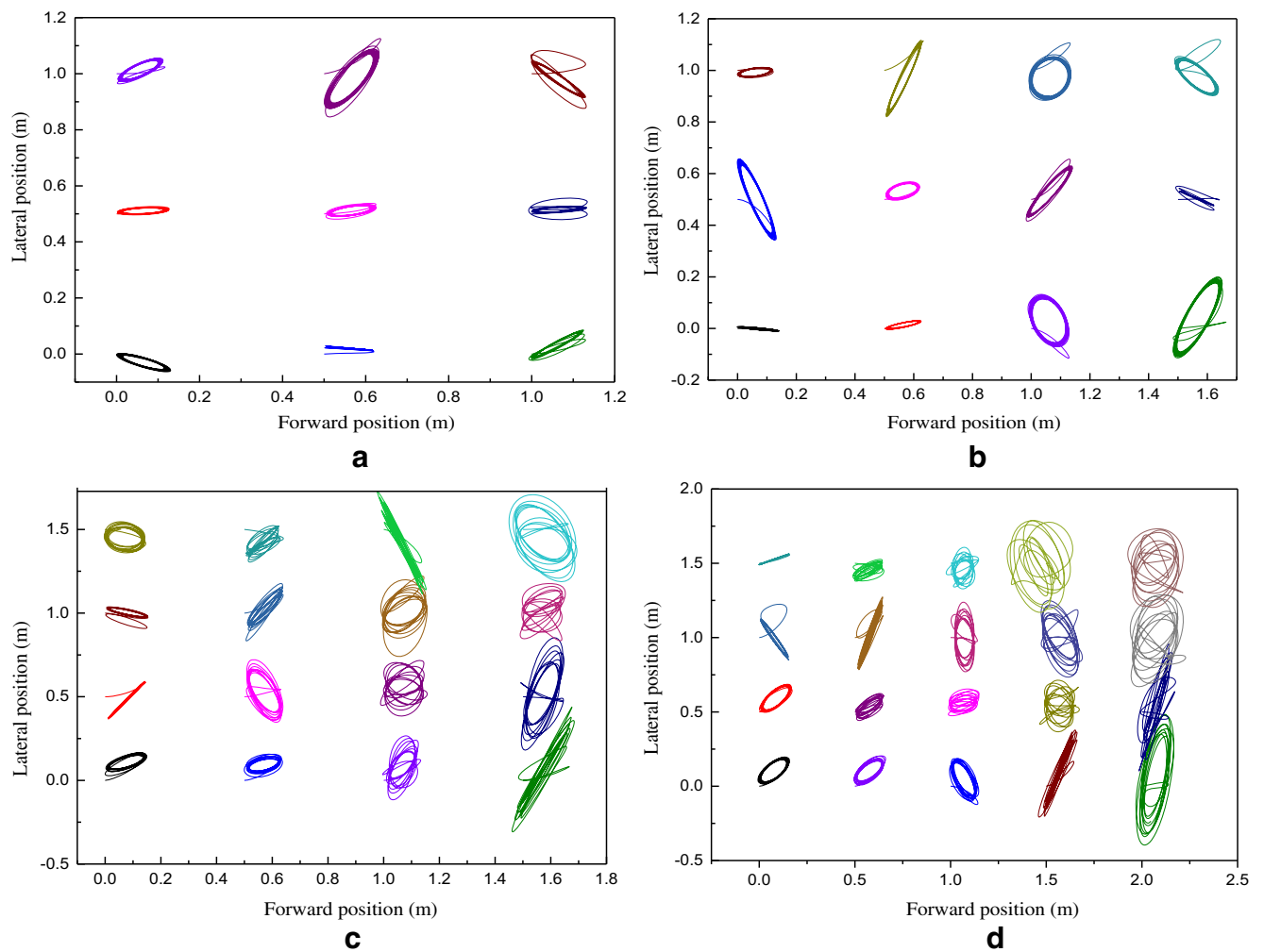


Fig. 11 Riser group vibration trajectory. (a) 9 risers. (b) 12 risers. (c) 16 risers. (d) 20 risers

scalable functions which can be dynamically connected to the Fluent solver. UDFs use standard C library functions and predefined macros and adjust the calculated values on a per

iteration basis. Due to the moving of solid-liquid boundary, the fluid grid must be changed, and the dynamic grid technique is needed. At this point, the dynamic and fixed mesh

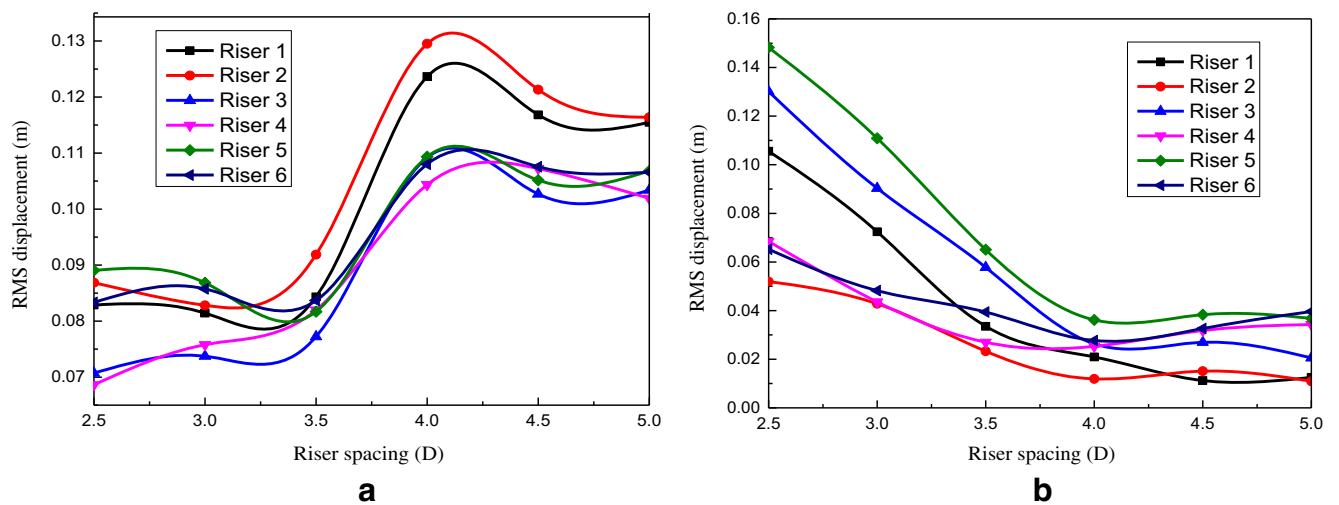


Fig. 12 Riser spacing—root mean square (RMS) amplitude. (a) Downstream. (b) Lateral

areas must be separated. The programming process flow of Fluent is very important when solving the fluid-solid coupling problem. Fluent must be the lead program for the whole process, as shown in Fig. 7.

Model verification

Based on literature review, experiments verifying the marine riser group flow-induced vibration numerical model have not been carried out. Therefore, in order to effectively verify the accuracy of this model, the vortex-induced vibration of a 3D elastic tube under cross-flow is calculated and compared with

the experimental results in Schowalter et al. (2006). The calculated input is consistent with the experimental conclusions (see Table 1). The flow field and grid are shown in Fig. 8 (x, fluid flow direction; y, lateral vibration direction of tube; z, axial direction of tube). A speed boundary is used for the left inlet, a pressure outlet boundary for the right outlet, and the other outer boundaries of the fluid field are set as fixed wall surfaces. The tube wall surface is a fluid-solid coupling interface, which is set as the boundary of the moving grid. The time step is 0.00025 s, and transient structural linearly loads the inlet flow rate to $U_r (= 0.5-10)$ within 0.05 s. Figure 9 respectively compares changes in the ratio f_{ex}/f_n between riser

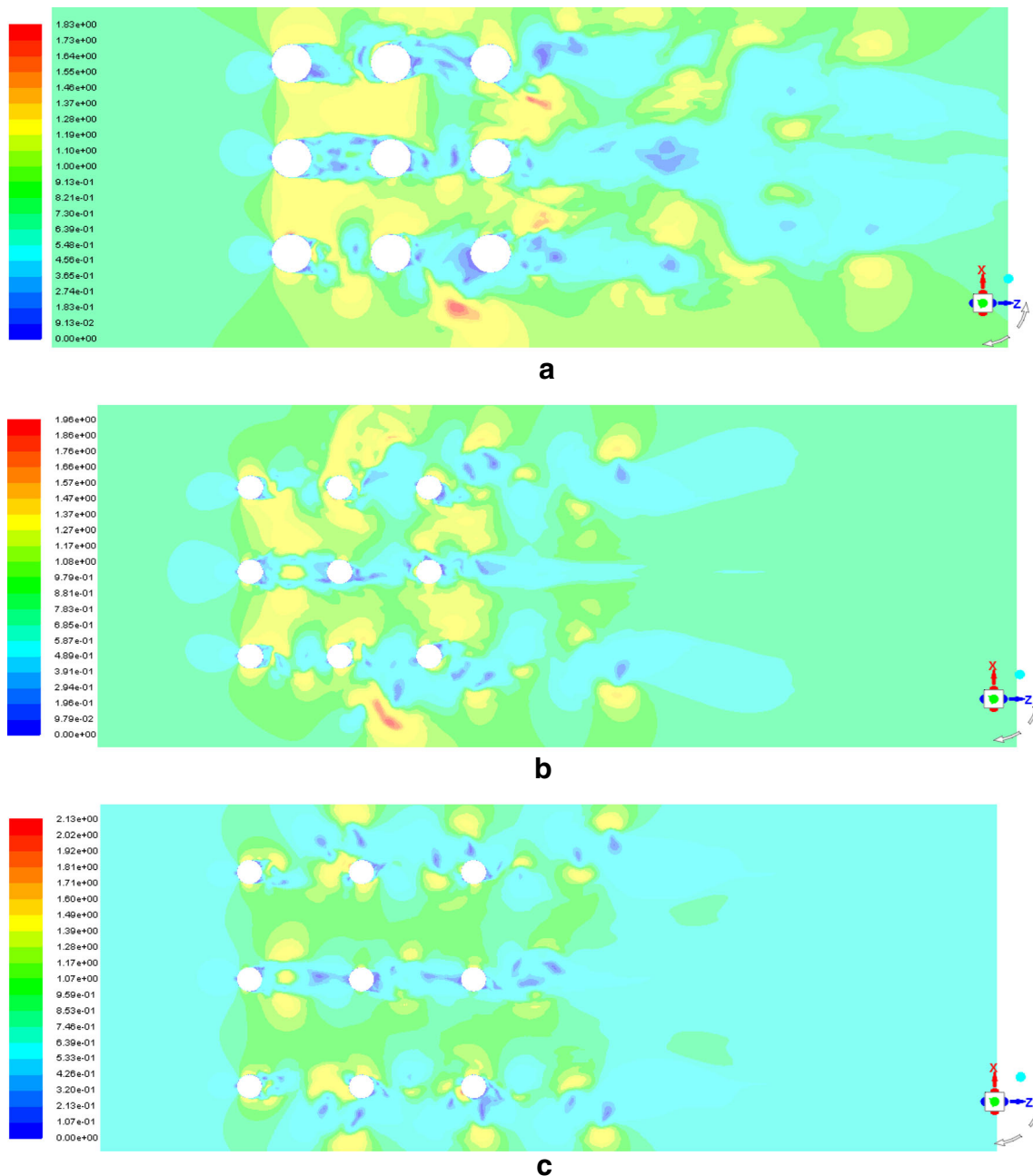


Fig. 13 Cloud maps of marine riser group spacing flow velocity fields. (a) Riser spacing of 2.5D. (b) Riser spacing of 3.5D. (c) Riser spacing of 4.5D

response frequency f_{ex} and natural frequency f_n and the lateral amplitude A_y/D and consequent flow velocity U_r obtained by numerical calculation, with the existing experimental results. It shows that the two agree well in terms of trends and values. Figure 10 a shows the calculated riser trajectory, which is consistent with the experimental results (Fig. 10b), indicating the accuracy of the model.

Analysis of multi-wellhead marine riser group vibration response characteristics

Based on the flow field-riser group structure numerical model, the vibration response characteristics of the riser group are analyzed under different factors, revealing their influence mechanisms on the vibration response and flow field motion of the riser group. The vibration patterns provide theoretical reference for the structural design of riser groups. The specific parameters of the model are shown in Table 2.

Effects of number of risers

Due to the two-way coupling between the riser and the fluid, the vortex-induced forms of the fluids and the effects on the riser group differ with different numbers of risers. Fluid-solid coupling dynamic response analysis was carried out for rectangular rows of 9, 12, 16, and 20 risers with external tube flow spacing of 4D and external fluid flow rate.

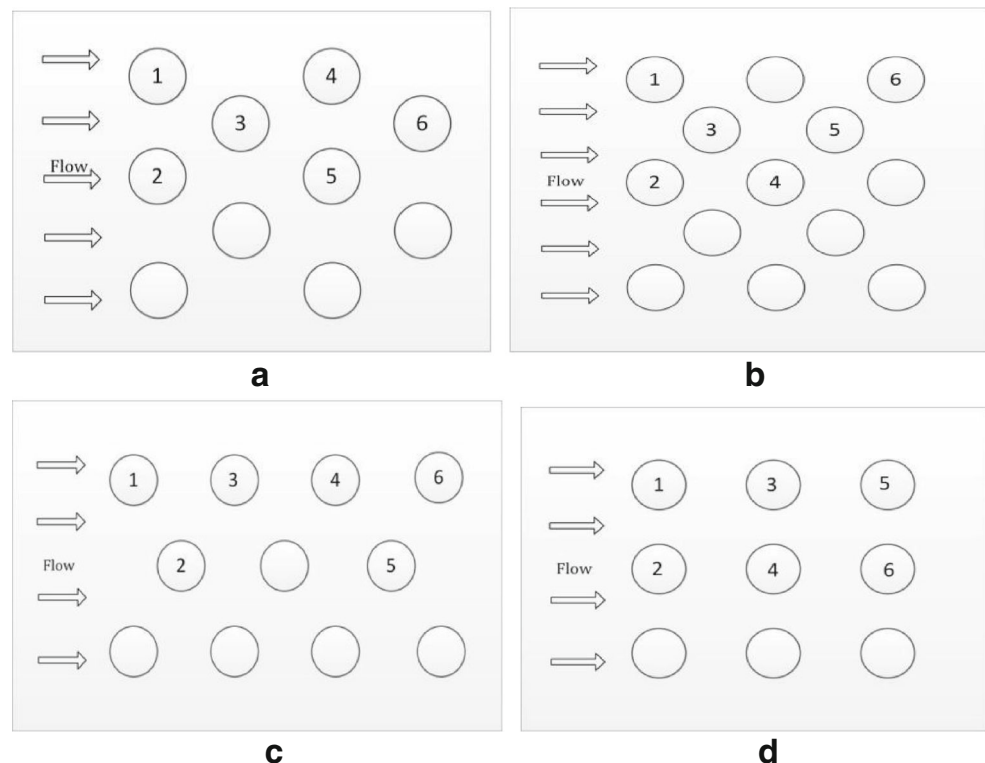
Figure 11 shows vibration trace diagrams with 9, 12, 16, and 20 risers. With a small number of risers, the main vibration direction of each is downstream, and the amplitude is essentially consistent. As the number increases, the main vibration direction of the first riser is downstream. The middle ones vibrate with equal amplitude, with significantly higher amplitude, and vibration becomes more extreme going downstream. Therefore, the effects of inflow and wake on the front and rear risers must be fully considered, particularly the wake disturbance of the rear riser.

Effects of riser spacing

In order to study the interaction within multi-wellhead riser groups and between risers, the dynamics of nine riser groups arranged as a square are analyzed. The distance S between the risers was 2.5D, 3D, 3.5D, 4D, 4.5D, and 5D, respectively, and the outflow rate is 0.8 m/s.

As shown in Fig. 12a, when the spacing is between 2.5D and 3.5D, the amplitude of the downstream flow of each riser does not change much, and the vibration is essentially stable. When the spacing increases to 3.5D–4D, the downstream vibration amplitude significantly increases for all risers. After the spacing is larger than 4D, the amplitude decreases slightly and gradually stabilizes. Thus, with spacing from 2.5D to 3.5D, the downstream interaction between the risers and the elastic force of the fluid inhibits vibration of the riser group; when the spacing is greater than 4D, the interaction is gradually weakened, so the

Fig. 14 Diagram of riser group arrangements. (a) Triangular arrangement. (b) Transposed square arrangement. (c) Transposed triangle arrangement. (d) Square arrangement



critical riser spacing in the downstream direction is $3.5D-4D$. As shown in Fig. 12b, the mutual interference within the riser group inhibits the lateral vibrations to a certain extent, with a critical distance around $3.5D-4D$.

Figure 13, flow field cloud maps of multi-wellhead marine riser groups at different intervals, shows that as the spacing increases, the velocity change region of the flow field is stable, and the interference between risers gradually decreases. When the spacing is $2.5D$, due to the shadow effect, the velocity downstream of the riser is relatively slow, so the drag force is also relatively small, and the forward vibration is insignificant. Due to the smaller spacing, however, the wake flow velocity distribution of the upstream risers is more turbulent, and the vortex radiation intensifies the lateral vibration of downstream risers. As the spacing increases, meanwhile, the forward-flow velocity gradually returns to its original state, so the vibration of downstream risers increases. Lateral vibration decreases, and the interaction between risers becomes insignificant. Therefore, different riser group spacing configurations based on site requirements

can effectively control vibration amplitude and the effects of the flow field on the riser group.

Effects of riser arrangement

In order to study the interaction within a multi-wellhead marine riser group, the vibration response characteristics of the group under different arrangements were analyzed. The distance S between the risers was $4D$, and the outflow velocity was 0.8 m/s .

Four arrangements were analyzed: an equilateral triangle (30°), transposed square (45°), transposed equilateral triangle (60°), and square (90°). In each of these arrangements, 6 risers are used as study objects. The arrangements are shown in Fig. 14.

(1) Effect of downstream vibration displacement

Figure 15 is a time-history curve of the riser group's forward vibration displacement under different arrangements. The figure shows that the riser vibration frequencies were

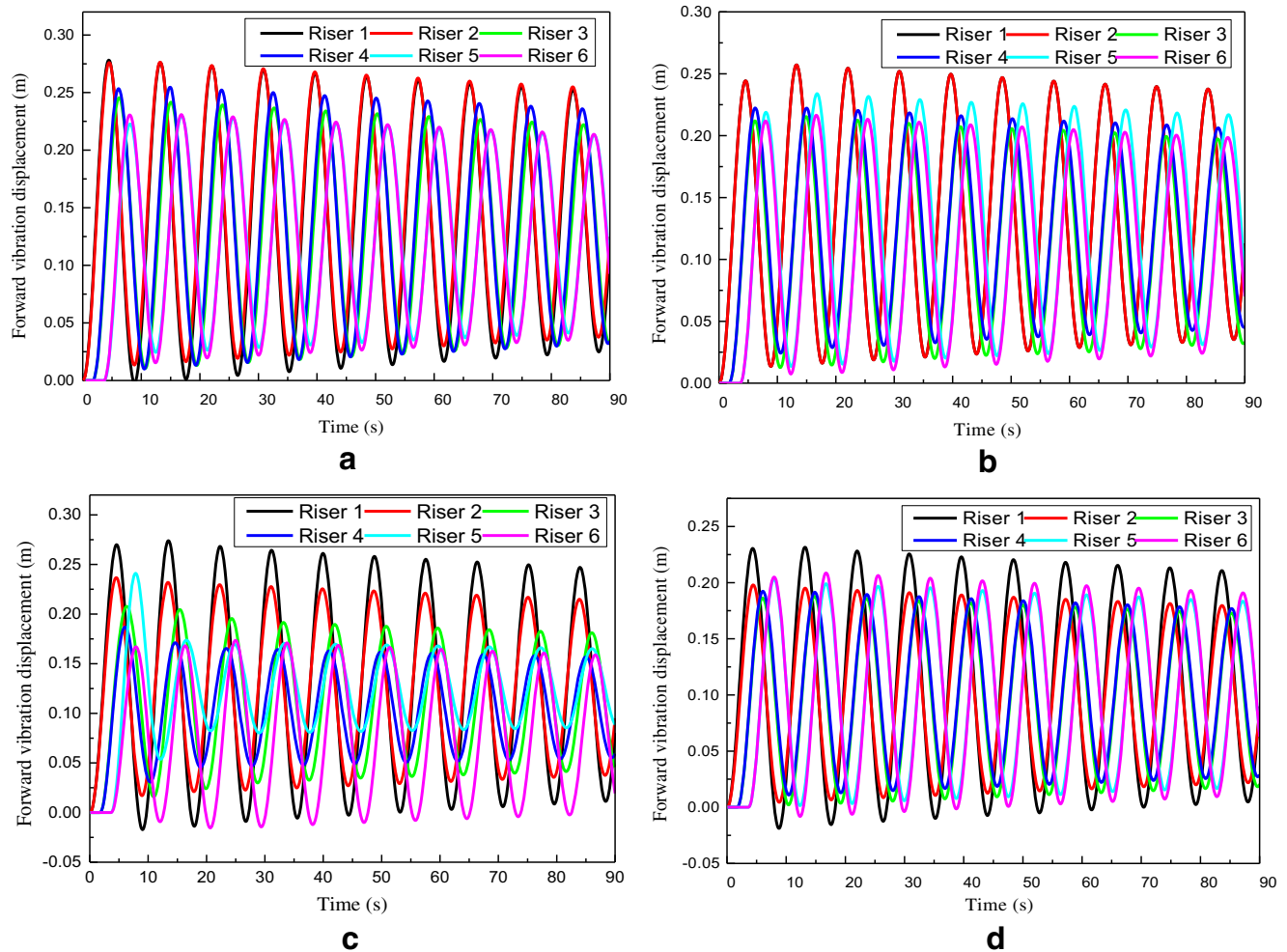


Fig. 15 Time-history vibration displacement diagram of riser group. (a) Triangular arrangement. (b) Transposed square arrangement. (c) Transposed triangle arrangement. (d) Square arrangement

similar in different arrangements, but the amplitudes were very different. Overall, the amplitude of the upstream risers is higher than for the downstream ones. When the angle between the riser groups is less than 45° , vibration of upstream and downstream risers must be considered simultaneously. When the angle is greater than 45° , the focus is on the vibration of the upstream riser.

(2) Effect of cross-flow on vibration displacement

Figure 16, the lateral vibrational displacement of the riser group under different arrangements, shows that the forward and lateral vibrations are similar in severity. The coupled vibration of both the forward and lateral flow must be considered when designing the riser structure. The vibrations of downstream risers are most severe when the arrangement is a transposed equilateral triangle or square. In other arrangements, the upstream risers vibrate most severely. Risers 1 and 2 vibrate in opposite directions at the same frequency, and the simultaneous separation and approach make accidents caused by riser collision very likely. Therefore, anti-collision devices

are necessary in the lateral direction to ensure the safe operation of the multi-wellhead riser group.

(3) Effects of flow field motion

Figure 17 a, the flow field velocity cloud diagram, shows that the downstream vortex wakes of the risers in the positive triangle arrangement interact, with strong mutual interference. Figure 17 b shows that in the transposed square arrangements, the vortex wakes between each layer of risers are independent of each other. The mutual interference is weak, and the flow field mainly affects the vibration of external risers. Figure 17 c shows that in this arrangement, when the lateral spacing is large, the interference between risers is small. A distinct vortex street appears, mainly influencing vibration in the downstream risers, and a “tail” phenomenon appears. Figure 17 d shows that the distance between risers in this arrangement partially inhibits the development of tail vortex streets, so that the fluid-elastic force acting on the risers is small. The riser vibration is also weaker in this arrangement than in the other ones.

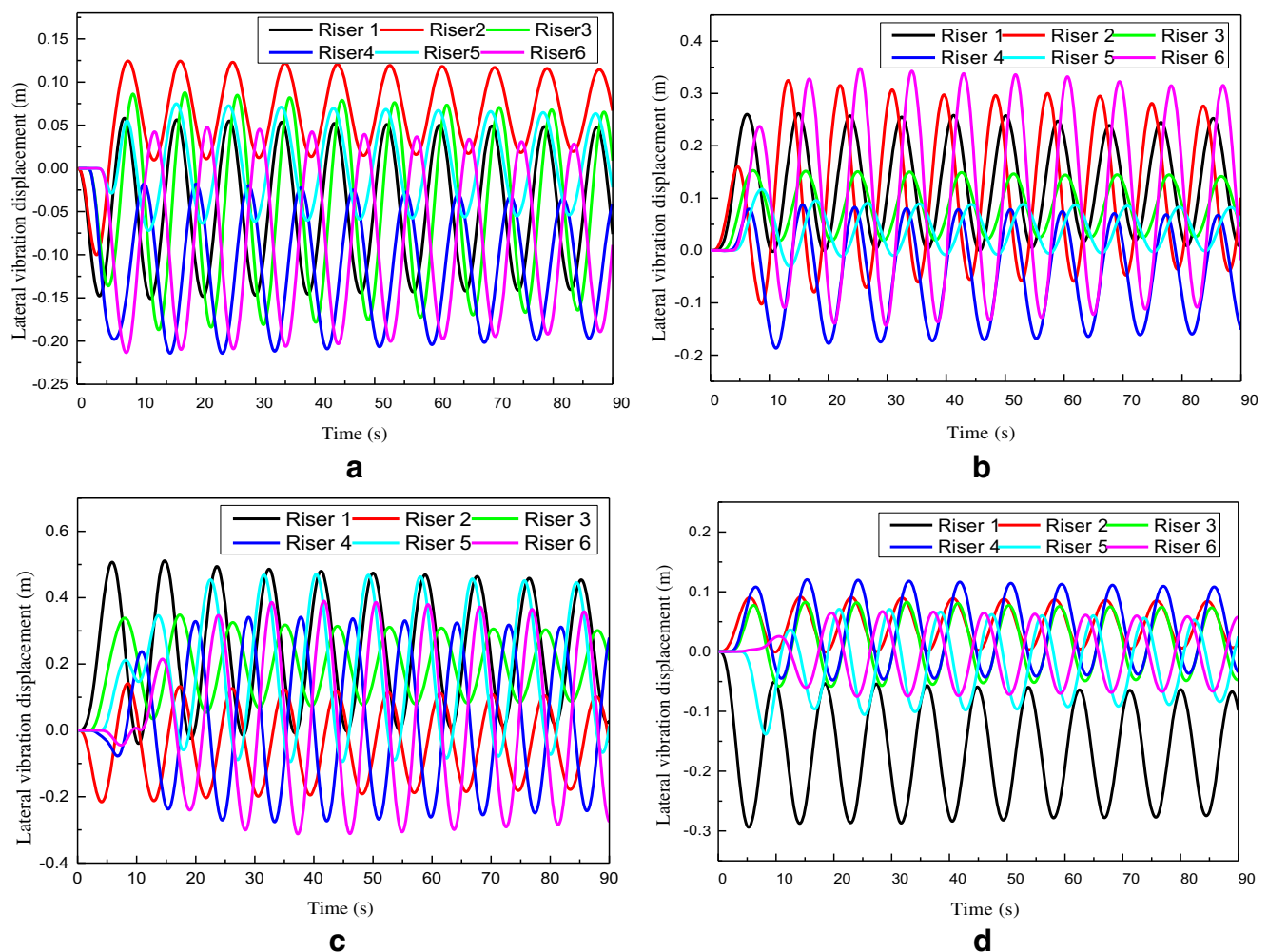
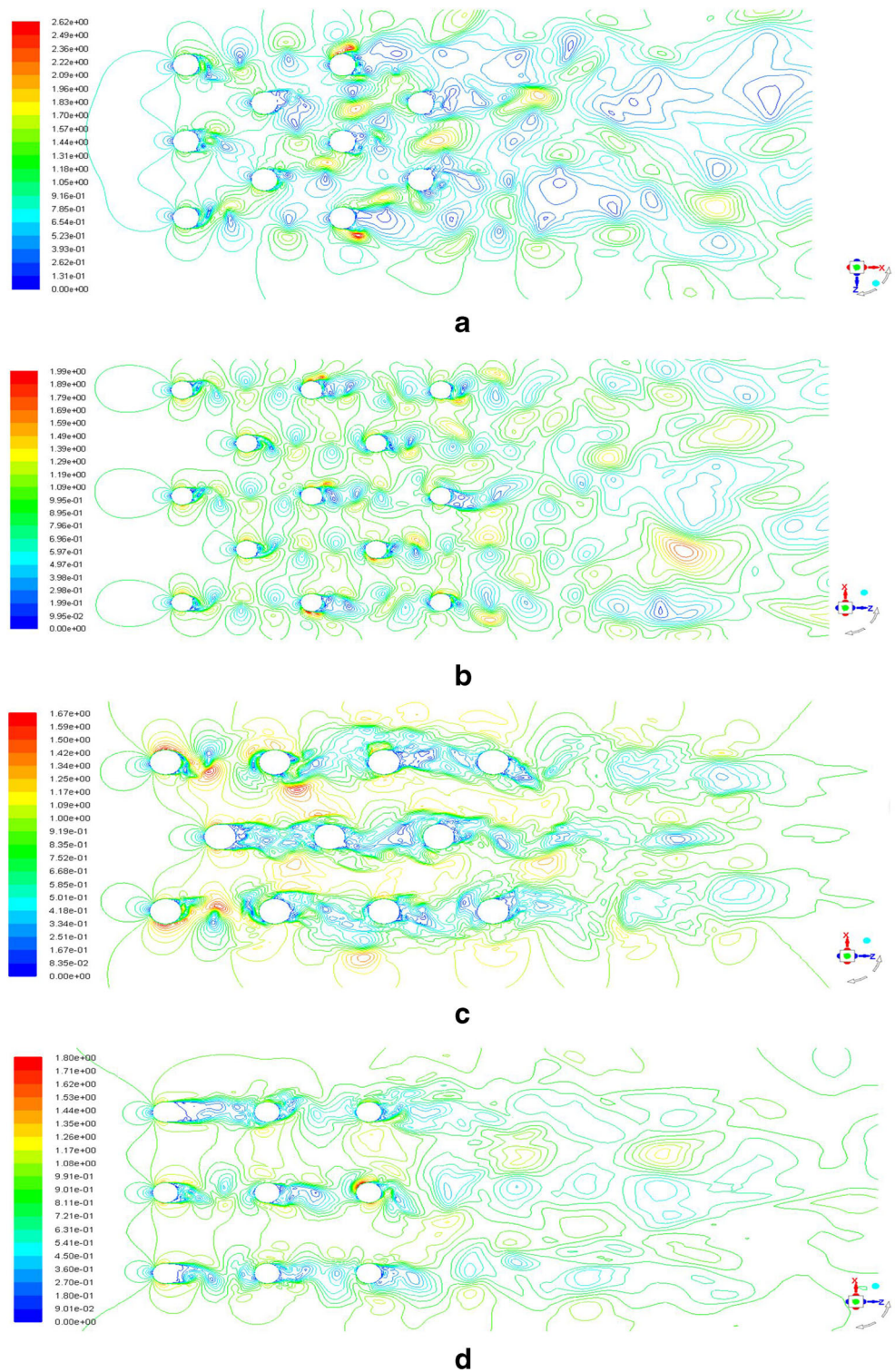


Fig. 16 Time-history vibration displacement diagram for each riser. (a) Triangular arrangement. (b) Transposed square arrangement. (c) Transposed triangle arrangement. (d) Square arrangement

Fig. 17 Flow field velocity map. (a) Triangular arrangement. (b) Transposed square arrangement. (c) Transposed triangle arrangement. (d) Square arrangement



Conclusion

In this paper, a numerical model and fluid turbulence model for forward-flow and the cross-flow coupling of marine riser groups are established for the problem of flow-induced vibration of multi-wellhead marine riser groups in uniform flow.

The model is used to analyze the effects of the number, spacing, and arrangement of riser groups on their vibration response characteristics, reaching the following conclusions:

- (1) Using computational fluid/solid dynamics (CFD/CSD), considering the simultaneous fluid-structure interaction

and the combination of ocean vortex force and wave force, a numerical model considering the coupled the coupled forward and lateral vibration of the riser group and a fluid turbulence model was established. A parallel coupling program was developed, and the numerical solution was performed using ANSYS Workbench and Fluent. In order to verify the accuracy of the model, the vibration response of a single riser was analyzed and compared with classic experimental analysis data.

- (2) The model was used to analyze the effects of riser number and spacing on the group's vibration characteristics. The analysis found that as the number of risers increases, the front row along the flow direction mainly vibrates in the forward direction, while the rear rows mainly vibrate laterally. Therefore, the incoming flow must be considered for the front row, while wake disturbance must be considered for the rear row. As the riser spacing increases, the mutual interference within the group significantly influences the forward and transverse flow; the critical spacing for interference is 3.5D–4D.
- (3) The model was used to analyze the effects of arrangement on the vibration characteristics, finding that the arrangement mainly affects lateral vibration; the influence on the upstream and downstream risers is most significant. The vibration response amplitude of the riser group appears to be the largest in a square arrangement. The triangular versus square arrangements directly influence the flow field-structure field coupling effect, and the effect is weaker in the latter.

Funding This work has been supported in part by the National Natural Science Foundation of China (Grant No. 51875489), National key R & D plan of China (2018YFC0310201), and Sichuan Province Youth Science and Technology Innovation Team (Grant No. 2019JDTD0017). Mr. Xiaoqiang Guo would like to acknowledge the financial support from the China Scholarship Council (Award No. 201908510191) for his 1-year visiting study at University of Regina.

References

- Antoine P, Sigrist JF (2009) Numerical simulation of an oscillating cylinder in a cross-flow at low Reynolds number: forced and free oscillations [J]. *Comput Fluids* 38:80–100
- Breuer M (1998) Numerical and modeling influences on large eddy simulations for the flow past a circular cylinder [J]. *Int J Heat Fluid Flow* 19(5):512–521
- Chaplin JR, Bearman PW, Huarte FJH et al (2005) Laboratory measurements of vortex-induced vibrations of a vertical tension riser in a stepped current [J]. *Journal of Fluids and Structures* 21(1):3–24
- Gao GH, Cui YJ, Qiu XQ et al (2019) Parameter influencing analysis of vortex-induced vibration response of deepsea top tensioned riser [J]. *Shipbuilding Engineering* 41(2):101–107
- Ge XB, Li YP, Shi XL, Chen XS, Ma HL, Yang CH, Shu C, Liu YX (2019) Experimental device for the study of Liquid-Solid coupled flutter instability salt cavern leaching tubing [J]. *Journal of Natural Gas Science and Engineering* 66:168–179
- Griffin OM, Ramberg SE (1982) Some recent studies of vortex-excited shedding with application to marine tubulars and risers [J]. *Journal of Energy Resources Technology* 104:2–13
- Gu JY, Yang C, Zhu XY et al (2016) Influences of mass ratio on vortex induced vibration characteristics of a circular cylinder [J]. *Journal of Vibration and Shock* 35(4):134–140
- He F, Dai HL, Huang ZH et al (2017) Nonlinear dynamics of a fluid-conveying pipe under the combined action of cross-flow and top-end excitations [J]. *Appl Ocean Res* 62:199–209
- Huang H. Multi-objective optimization design based on interference analysis of top-tensioned riser [D]. Dalian University of Technology, 2010.
- Huse E, Kleiven G. Impulse and Energy in Deepsea Riser Collisions Owing to Wake Interference [C]// 2000.
- Jauvtis N, Williamson CHK (2003) Vortex-induced vibration of a cylinder with two degrees of freedom [J]. *Journal of Fluids and Structures* 17(7):1035–1042
- Leonard BP (1991) The ultimate conservative difference scheme applied to unsteady one-dimensional advection [J]. *Comput Methods Appl Mech Eng* 88:17–74
- Liu J, Guo XQ, Liu QY, Wang GR, He YF, Li J (2019) Analysis of vortex induced vibration response characteristics of marine riser considering the in-line and cross-flow coupling effect [J]. *Acta Pet Sin* 40(10):1270–1280
- Liu J, Guo X, Wang G et al (2020) Bi-nonlinear vibration model of tubing string in oil&gas well and its experimental verification [J]. *Appl Math Model* 81:50–69
- Sang S, Chu ZF, Cao AX et al (2019) Vortex-parametric coupled vibration characteristics of Deep-Sea top-tension riser [J]. *Journal of Harbin University of Engineering*:1–6
- Schowalter D, Ghosh I, Kim S E, et al. Unit-tests based validation and verification of numerical procedure to predict vortex-induced motion [C]. 25th International Conference on Offshore Mechanics and Arctic Engineering, Hamburg, 2006.
- Shi Y, Zhou XD, Cao J et al (2015) Intervention analysis of tension leg platform top tension riser under wave and current action [J]. *Marine engineering equipment and technology* 2(2):84–87
- Song Q, Zhang WG, Chang YJ et al (2016) Analysis of Interference Factors for TLP Riser System [J]. *Petroleum Machinery* 44(3):51–57
- Su MD, Huang SY (1997) *Computational Fluid Dynamics Foundation* [M]. Tsinghua University Press, Beijing
- Xu J, Wang DS, Huang H et al (2017) A vortex-induced vibration model for the fatigue analysis of a marine drilling riser [J]. *Ships and Offshore Structures* 12(S1):S280–S287
- Yan Y. Study on Numerical Simulation of deepwater riser collision [D]. Dalian University of Technology, 2010.
- Zdravkovich MM (1997) Flow around circular cylinders [J]. *Fundamentals* 1(1):216
- Zhang Z S, Cui G X, Xu C X. Turbulence theory and simulation [M]. Beijing: tsinghua university press, 2005.
- Zhang Q, Yang HB, Huang Y et al (2012) Effect of Several Key Parameters on the Dynamic Analysis of TTR [J]. *Marine mechanics* 16(3):296–306
- Zhou WW, Cao J, Zhang EY (2016) Study on Interference Effect of Top Tension Riser in the Extreme Soliton Current [J]. *Oil Field Equipment* 45(6):1–6
- Zhu XH, Li B, Liu QY, Chang XJ, Li LC, Zhu KL, Xu XF (2015) New Analysis Theory and Method for Drag and Torque Based on Full-Hole System Dynamics in Highly Deviated Well [J]. *Math Probl Eng*